

translocation of the biotin ring could be accomplished through allowed rotations about two single bonds of the side chain.<sup>40</sup> The minimal migration model received strong support from the observation that transcarboxylase catalyzes a small amount of <sup>3</sup>H transfer between pyruvate and propionyl CoA.<sup>44</sup> If, as seems reasonable on mechanistic grounds, the OH proton of the enol form of biotin is the proton carrier, the diffusion-limited exchange of this proton with solvent<sup>16,33,28</sup> requires a rapid rate of migration

(44) I. A. Rose, E. L. O'Connell, and F. Solomon, *J. Biol. Chem.*, **251**, 902 (1976).

of the biotin enol between the two bound substrates, consistent with minimal movement of the biotin ring.

**Acknowledgment.** We are grateful to Ronald Breslow, Irwin A. Rose, William P. Jencks, and R. Parthasarathy for their helpful comments on this work.

(45) J. A. Glasel, *Biochemistry*, **5**, 1851 (1966).

(46) Differing exchange rates with ethanol of the two unassigned NH protons of biotin methyl ester in chloroform were qualitatively noted by their unequal line broadenings.<sup>45</sup> In accord with our assignments, the upfield resonance exchanged more rapidly.

## Cobalt(II) Nitrosyl Cation Radicals of Porphyrins, Chlorins, and Isobacteriochlorins. Models for Nitrite and Sulfite Reductases and Implications for A<sub>1u</sub> Heme Radicals

Etsuko Fujita, C. K. Chang,<sup>1</sup> and Jack Fajer\*

Contribution from the Department of Applied Science, Brookhaven National Laboratory, Upton, New York 11973, and the Department of Chemistry, Michigan State University, East Lansing, Michigan 48824. Received February 13, 1985

**Abstract:** Oxidation of cobalt(II) nitrosyl complexes of porphyrins (P), chlorins (C), and isobacteriochlorins (iBC) yields Co<sup>III</sup>NO  $\pi$ -cation radicals. The radicals are stable and recyclable to the parent compound without loss of NO. The oxidized species have been characterized by electrochemistry, visible and infrared spectroscopy, and electron spin resonance (ESR). Interest in these intermediates is prompted by the presence of iron Cs or iBCs in enzymes that catalyze the reductions of nitrite to ammonia or nitric oxide (nitrite reductases) and the recent identification of cobalt iBC in sulfite reductases, enzymes which are also capable of nitrite reduction. The optical spectra of the Co<sup>III</sup>NO radicals resemble those previously obtained on oxidation of Fe<sup>II</sup>NOC and iBC and lend support to the assignment of those ESR-silent species as Fe<sup>II</sup>NOC<sup>+</sup> and iBC<sup>+</sup>  $\pi$ -cation radicals. As found in other series with the same macrocycles (Fe<sup>II</sup>NO, Fe<sup>II</sup>Cl, Zn, H<sub>2</sub>), the Co<sup>II</sup>NO complexes become progressively easier to oxidize as the porphyrin is saturated (P < C < iBC, easiest). In all three species, the Co-NO bonds remain bent, suggestive of some Co-NO<sup>-</sup> character. The C and iBC radicals exhibit ESR features characteristic of "a<sub>1u</sub>" radicals that include spin delocalization onto the metal. Similar spin profiles may rationalize the ESR spectra of presumed "a<sub>1u</sub>" porphyrin radicals in oxidized chloroperoxidase, catalase, and cytochrome P450.

Prosthetic groups comprised of iron isobacteriochlorins (sirohemes) and chlorins (hemes d) have been identified in several enzymes that catalyze the multielectron reduction of nitrite to ammonia<sup>2</sup> (assimilatory nitrite reductases, sirohemes) or its one-electron reduction to nitric oxide<sup>3</sup> (dissimilatory reductases, hemes d). The possibility that Fe<sup>II</sup>NO complexes occur in the catalytic cycles of the enzymes<sup>4</sup> led us<sup>5</sup> to a comparative study of the redox chemistry of Fe<sup>II</sup>NO complexes of porphyrins (P), chlorins (C), and isobacteriochlorins (iBC). No distinctive features that favored the biological selection of one macrocycle over the others were found either in their reduction potentials or in the binding of NO. However, the progressive saturation of the porphyrin framework made their Fe<sup>II</sup>NO complexes easier to oxidize, resulting in a shift from metal-centered oxidation in the porphyrin to macrocycle oxidations in the chlorin and isobacteriochlorin. The NO substrate became less labile in the oxidized C than in P, and still less in iBC. The Fe-NO bond remained bent in the oxidized C and iBC but was linear in the P. Because linear and bent M-NO bonds may be formally considered<sup>6</sup> as M-NO<sup>+</sup> and M-NO<sup>-</sup>, respectively, a bent Fe-NO bond may therefore be more susceptible to protolytic reactions that eventually generate ammonia in the sirohemes. If electron transport in the enzymic cycle occurs via oxidized macrocycle transients, as previously suggested,<sup>7,8</sup> then the biological choice of macrocycle would thus allow control of oxidation site (metal

vs. macrocycle) and of the reactivity and residence time of the NO substrate at the catalytic site.

Our conclusions<sup>5,9</sup> regarding the Fe<sup>III</sup>NOP<sup>+</sup> species, reached on spectroscopic evidence, were confirmed by Scheidt et al.,<sup>10</sup> who

(1) Michigan State University.

(2) Siegel, L. M.; Murphy, M. J.; Kamin, H. *J. Biol. Chem.* **1973**, *248*, 251-264. Murphy, M. J.; Siegel, L. M.; Kamin, H. *Ibid.* **1973**, *248*, 2801-2814. Murphy, M. J.; Siegel, L. M.; Tove, S. R.; Kamin, H. *Proc. Natl. Acad. Sci. U.S.A.* **1974**, *74*, 612-616. Vega, J. M.; Garret, R. H. *J. Biol. Chem.* **1975**, *250*, 7980-7989. Huckelsby, D. P.; James, D. M.; Banwell, M. J.; Hewitt, E. J. *Phytochemistry* **1976**, *15*, 599-603.

(3) Horie, S.; Watanabe, T.; Nakamura, S. *J. Biochem.* **1976**, *80*, 579-593. Kim, C. H.; Hollocher, T. C. *J. Biol. Chem.* **1983**, *258*, 4861-4863.

(4) Lancaster, J. R.; Vega, J. M.; Kamin, H.; Orme-Johnson, N. R.; Orme-Johnson, W. H.; Krueger, R. J.; Siegel, L. M. *J. Biol. Chem.* **1979**, *254*, 1268-1272. Johnson, M. K.; Thomson, A. J.; Walsh, T. A.; Barber, D.; Greenwood, C. *Biochem. J.* **1980**, *189*, 285-294.

(5) Fujita, E.; Fajer, J. *J. Am. Chem. Soc.* **1983**, *105*, 6743-6745.

(6) McCleverty, J. A. *Chem. Rev.* **1979**, *79*, 53-76.

(7) Stolzenberg, A. M.; Spreer, L. O.; Holm, R. H. *J. Chem. Soc., Chem. Commun.* **1979**, 1077-1078. Stolzenberg, A. M.; Spreer, L. O.; Holm, R. H. *J. Am. Chem. Soc.* **1980**, *102*, 364-370. Stolzenberg, A. M.; Strauss, S. M.; Holm, R. H. *Ibid.* **1981**, *103*, 4763-4775.

(8) Richardson, P. F.; Chang, C. K.; Spaulding, L. D.; Fajer, J. *J. Am. Chem. Soc.* **1979**, *101*, 7736-7738. Chang, C. K.; Fajer, J. *Ibid.* **1980**, *102*, 848-851. Richardson, P. F.; Chang, C. K.; Hanson, L. K.; Spaulding, L. D.; Fajer, J. *J. Phys. Chem.* **1979**, *83*, 3420-3424. Chang, C. K.; Hanson, L. K.; Richardson, P. F.; Young, R.; Fajer, J. *Proc. Natl. Acad. Sci. U.S.A.* **1981**, *78*, 2652-2656.

(9) A similar conclusion was reached by Lancon and Kadish: Lancon, D.; Kadish, K. M. *J. Am. Chem. Soc.* **1983**, *105*, 5610-5617.

(10) Scheidt, W. R.; Lee, Y. J.; Hatano, K. *J. Am. Chem. Soc.* **1984**, *106*, 3191-3198.

\* Address correspondence to this author at Brookhaven National Laboratory.

determined the X-ray structure of  $\text{Fe}^{\text{III}}\text{OEP}(\text{NO})\text{ClO}_4$ . The ferric ion is low spin, the Fe-NO bond is linear, and the NO is easily lost.

Although the optical and redox data for the oxidized C and iBC complexes strongly suggested the existence of  $\pi$  cations, the species were ESR silent, presumably because of spin pairing between the radicals and the  $\text{Fe}^{\text{II}}\text{NO}$ .<sup>5</sup> Unlike neutral  $\text{Fe}^{\text{II}}\text{NO}$  complexes,  $\text{Co}^{\text{II}}\text{NO}$  porphyrins are diamagnetic<sup>11</sup> and therefore should yield paramagnetic products on oxidation. We report here an extension of our previous work to  $\text{Co}^{\text{II}}\text{NO}$  complexes. Redox trends similar to those of the iron compounds are observed; the existence of  $\text{Co}^{\text{II}}\text{NO}$  iBC and C  $\pi$  cations is established by ESR, and optical similarities between the Co radicals and the Fe iBC and C support the radical formulation proposed for the iron species. In addition, oxidation of  $\text{Co}^{\text{II}}\text{NOP}$  also leads to a  $\pi$  cation, unlike the ferrous porphyrin which is oxidized to  $\text{Fe}^{\text{III}}$ . As in the  $\text{Fe}^{\text{II}}$  radicals, the Co-NO bonds remain bent.

Besides serving as a spectroscopic probe, the substitution of cobalt for iron may also be biologically relevant. Some sulfite reductases, which reduce sulfite to hydrogen sulfide and can also reduce nitrite, have recently been shown to contain cobalt iBC.<sup>12</sup>

The  $\text{CoNOiBC}$  and C ESR results may also be relevant in a different context. The spectra yield good agreement with spin profiles theoretically predicted for " $a_{1u}$ " radicals<sup>8,13-16</sup> but clearly require some magnetic interaction of the radical with the metal.  $A_{1u}$  porphyrin radicals have been invoked to explain the spectral features of the oxidized heme transients (compounds I) of catalase<sup>17</sup> and chloroperoxidase.<sup>16</sup> Although the iron-radical coupling for the latter has been judged<sup>18</sup> too strong to be consistent with the proposed  $a_{1u}$  assignment, the results presented here for the cobalt C and iBC radicals certainly demonstrate coupling between some  $a_{1u}$  radicals and the metal they bind.

### Experimental Section

ESR spectra were recorded on a Bruker-IBM ER200D spectrometer equipped with a field frequency lock and an Aspect 2000 data system. Radicals were generated electrolytically in "vacuum cells".<sup>15</sup> ESR samples were fitted with optical cells<sup>15</sup> to allow monitoring before and after ESR measurements. The techniques used for solvent and electrolyte purification and for controlled-potential electrolyses have been described.<sup>15,19</sup> Cyclic voltammograms were obtained with an IBM EC 225 voltammetric analyzer with use of a microcell<sup>20</sup> under a  $\text{N}_2$  atmosphere. For infrared measurements, samples were prepared by vacuum electrolysis, the identity of the product confirmed by visible spectroscopy, and the solvent removed by vacuum distillation. Nujol mulls of the residue, radical and electrolyte, were prepared under  $\text{N}_2$  immediately before the IR measurements. The electrolytes, tetrabutyl- or tetrapropylammonium perchlorate, do not interfere in the region of interest: 1500-1950  $\text{cm}^{-1}$ .

*trans*-Octaethylchlorin ( $\text{H}_2\text{OEC}$ ),<sup>21</sup> methyloctaethylchlorin ( $\text{H}_2\text{MeOEC}$ ),<sup>21</sup> octaethylisobacteriochlorin ( $\text{H}_2\text{OEiBC}$ ),<sup>21</sup> and the three

(11) Scheidt, W. R.; Hoard, J. L. *J. Am. Chem. Soc.* **1973**, *95*, 8281-8286.  
(12) Moura, J. J. G.; Moura, I.; Bruschi, M.; LeGall, J.; Xavier, A. V. *Biochem. Biophys. Res. Commun.* **1980**, *92*, 962-970. Hatchikian, E. C. *Ibid.* **1981**, *103*, 521-530. Battersby, A. R.; Sheng, Z. C. *J. Chem. Soc., Chem. Commun.* **1982**, 1393-1394.

(13) For simplicity, the  $a_{1u}$  and  $a_{2u}$  terminology<sup>14</sup> for porphyrins with  $D_{4h}$  symmetry will also be used for Cs and iBCs.

(14) Fajer, J.; Davis, M. S. "The Porphyrins"; Dolphin, D., Ed.; Academic Press: New York, 1979; Vol. 4, pp 197-256.

(15) Fajer, J.; Fujita, I.; Davis, M. S.; Forman, A.; Hanson, L. K.; Smith, K. M. *Adv. Chem. Ser.* **1982**, *201*, 489-513.

(16) Hanson, L. K.; Chang, C. K.; Davis, M. S.; Fajer, J. *J. Am. Chem. Soc.* **1981**, *103*, 663-670.

(17) Dolphin, D.; Forman, A.; Borg, D. C.; Fajer, J.; Felton, R. H. *Proc. Natl. Acad. Sci. U.S.A.* **1971**, *68*, 614-618.

(18) Schulz, C. E.; Rutter, R.; Sage, J. T.; Debrunner, P. G.; Hager, L. P. *Biochemistry* **1984**, *23*, 4743-4754.

(19) Fajer, J.; Brune, D. C.; Davis, M. S.; Forman, A.; Spaulding, L. D. *Proc. Natl. Acad. Sci. U.S.A.* **1975**, *72*, 4956-4960.

(20) Fujita, I.; Chang, C. K. *J. Chem. Educ.* **1984**, *61*, 913.

(21) Abbreviations used are the following: OEP, 2,3,7,8,12,13,17,18-octaethylporphyrin; OEC, *trans*-2,3-dihydro-2',3',7,8,12,13,17,18-octaethylporphyrin; MeOEC, 2-hydro-2'-methyl-3,3',7,8,12,13,17,18-octaethylporphyrin; 2,3-DMeOEiBC, 3,7-dimethyl-3',7'-dihydro-2',2',8,8',12,13,17,18-octaethylporphyrin; 1,4-DMeOEiBC, 2,8-dimethyl-2',8'-dihydro-3,3',7,7',12,13,17,18-octaethylporphyrin; 2,4-DMeOEiBC, 3,8-dimethyl-3',8'-dihydro-2,2',7,7',12,13,17,18-octaethylporphyrin; TPP, 5,10,15,20-tetraphenylporphyrin.

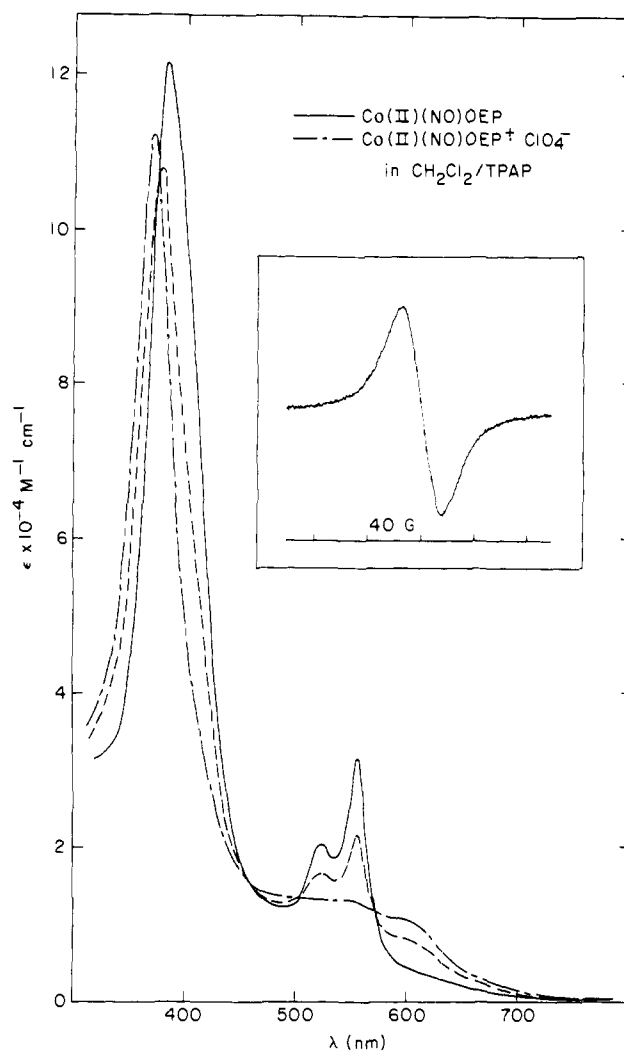


**Figure 1.** Optical changes that accompany the electrooxidation of cobalt(II) nitrosyl octaethylporphyrin (—) to its cation radical (---). The spectra develop with well-defined isobestic points but only one intermediate curve is shown (---). ( $T = 25^\circ\text{C}$ .) The insert shows the first derivative ESR spectrum of the radical. ( $T = 20^\circ\text{C}$ ,  $g = 2.0028$ .) The solvent is  $\text{CH}_2\text{Cl}_2$  and the electrolyte  $(\text{C}_3\text{H}_7)_4\text{NClO}_4$ .

isomers of dimethyloctaethylisobacteriochlorin ( $\text{H}_2\text{DMeOEiBC}$ )<sup>21</sup> were prepared by published methods.<sup>7,8,22</sup> Octaethylporphyrin ( $\text{H}_2\text{OEP}$ ),<sup>21</sup> purchased from Strem Chemicals, was used without further purification. Deuterium was incorporated at the meso positions (5,10,15,20- $\text{H}_2\text{OEP-d}_4$ ) with  $\text{D}_2\text{SO}_4\text{-D}_2\text{O}$ .<sup>23</sup> Cobalt was inserted into the porphyrin and the chlorins by refluxing the free base and cobalt acetate in acetic acid under a  $\text{N}_2$  atmosphere. The precipitated products were washed with  $\text{H}_2\text{O}$  and dried. Co iBCs were prepared in pyridine, the solvent evaporated, and the products washed with  $\text{H}_2\text{O}$  under a  $\text{N}_2$  atmosphere. Nitrosyl complexes were prepared on a vacuum line by exposure of the  $\text{Co}^{\text{II}}$  compounds dissolved in a few milliliters of  $\text{CH}_2\text{Cl}_2$  containing  $\sim 10\%$  EtSH to  $\sim 1$  atm of NO, followed by vacuum distillation to remove solvent and reagents. The ampule containing the  $\text{Co}^{\text{II}}\text{NO}$  product was then sealed and connected to an electrolytic cell through a break seal.  $^{15}\text{NO}$  (98%  $^{15}\text{N}$ ) was purchased from Merck and Co.

### Results and Discussion

The redox behavior of the  $\text{Co}^{\text{II}}\text{NO}$  compounds parallels that found previously for the  $\text{Fe}^{\text{II}}\text{NO}$  complexes;<sup>5</sup> the oxidations become progressively easier as the macrocycles are saturated:  $E_{1/2} = 0.77$  (OEP), 0.48 (OEC), and 0.24 V (OEiBC) in  $\text{CH}_2\text{Cl}_2$  vs. SCE (similar values  $\pm 0.02$  V are obtained in butyronitrile). Similar

(22) Chang, C. K. *Biochemistry* **1980**, *19*, 1971-1976.

(23) Smith, K. M. "Porphyrins and Metalloporphyrins"; Elsevier Publishing Co.: Amsterdam, 1975; p 816.

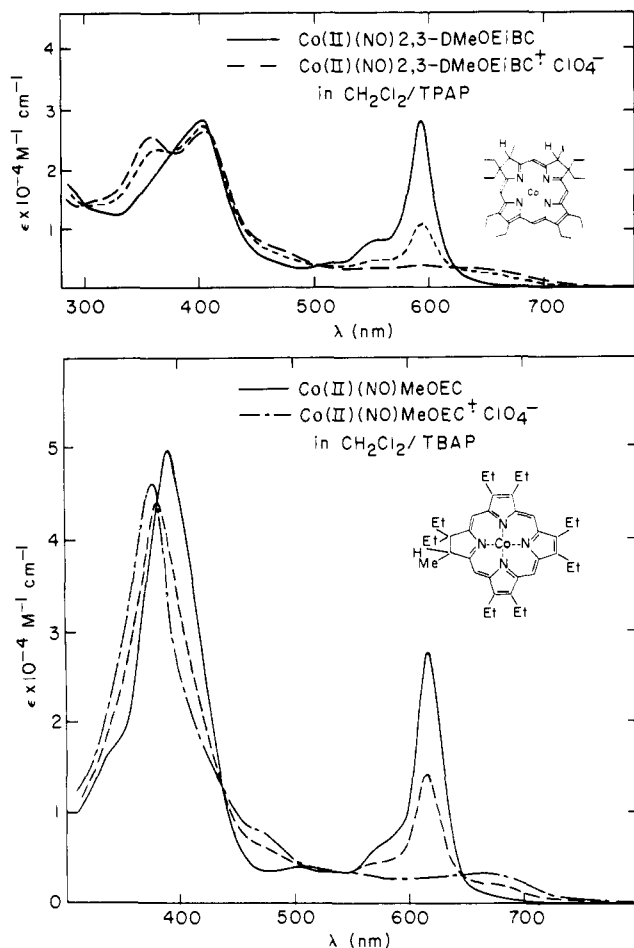


**Figure 2.** Optical changes observed on oxidation of (top) cobalt(II) nitrosyl 2,3-dimethyloctaethylisobacteriochlorin (—) to its cation radical (---) and (bottom) of cobalt(II) nitrosyl methyloctaethylchlorin (—) to its radical (---). One intermediate curve is shown in each case. The solvent is  $\text{CH}_2\text{Cl}_2$  and the electrolytes  $(\text{C}_3\text{H}_7)_4\text{NClO}_4$  and  $(\text{C}_4\text{H}_9)_4\text{NClO}_4$  for the iBC and C, respectively. ( $T = 25^\circ\text{C}$ .)

trends have been observed<sup>7,8</sup> in the P, C, iBC series in free bases, Zn,  $\text{Co}^{\text{III}}$ ,<sup>24</sup>  $\text{Fe}^{\text{III}}\text{Cl}$ ,  $\text{Fe}^{\text{II}}\text{CO}$  and NO complexes, and have been advanced<sup>5,7,8</sup> as possible reasons for the natural selection of iBCs. The oxidation shifts are predicted theoretically: the highest occupied  $\pi$  orbitals rise with saturation of the porphyrin skeleton, and oxidations that lead to  $\pi$  cations become easier and favored.<sup>8</sup>

In contrast to this behavior, reduction of the  $\text{Co}^{\text{II}}\text{NO}$  complexes is effectively independent of macrocycle:  $E_{1/2} = -1.26$  (OEP),  $-1.26$  (OEC), and  $-1.29$  V (OEiBC) in butyronitrile. This behavior again parallels that of the  $\text{Fe}^{\text{II}}\text{NO}$  series in which reduction is presumed to add an electron to a hybrid Fe-NO orbital.<sup>5</sup> The reductions of the  $\text{Co}^{\text{II}}\text{NO}$  species are reversible on a cyclic voltammetric time scale (seconds), but the porphyrin loses its NO during controlled-potential electrolysis in butyronitrile, to yield  $\text{Co}^{\text{I}}\text{OEP}^-$ , in agreement with results obtained by Kadish and co-workers<sup>25</sup> for  $\text{Co}^{\text{II}}\text{NOTPP}$ <sup>21</sup> in coordinating solvents. Unlike the porphyrin,  $\text{CoNOiBC}$  reduces to a stable product<sup>26</sup> that can be reoxidized to the parent nitrosyl.

These differences further illustrate the significant influence that the macrocycle can exert on the stability of the metal-nitrosyl bond following redox reactions in both the cobalt- and iron-NO

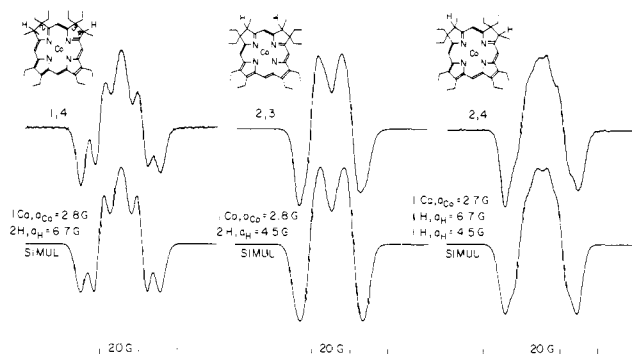


**Figure 3.** Second-derivative ESR spectra, in  $\text{CH}_2\text{Cl}_2$ , of the  $\pi$ -cation radicals of the 1,4- (left), 2,3- (middle), and 2,4- (right) dimethyloctaethyl(iBC) complexes of  $\text{Co}^{\text{II}}\text{NO}$ . ( $T = 20^\circ\text{C}$ ,  $g = 2.0057$ .) The simulations shown under the experimental spectra demonstrate that one cobalt and two protons on the saturated rings determine the spectral patterns observed.

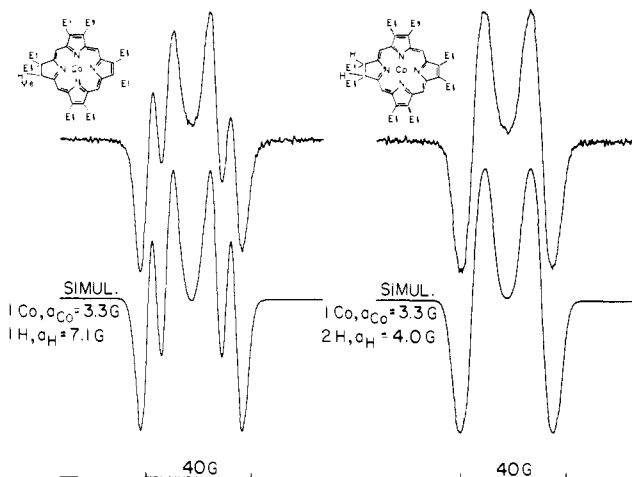


**Figure 4.** Second-derivative ESR spectra, in  $\text{CH}_2\text{Cl}_2$ , of the  $\pi$ -cation radicals of (left) the methyloctaethyl- and (right) octaethylchlorin complexes of  $\text{Co}^{\text{II}}\text{NO}$ . ( $T = 20^\circ\text{C}$ ,  $g = 2.0026$ .) The simulations duplicate the experimental features with one cobalt and one (MeOEC) or two (OEC) protons.

species. Structurally, hydroporphyrins (Cs, iBCs, and bacteriochlorins) tend to be more flexible, with longer metal-to-pyrrole nitrogen distances than porphyrins;<sup>27,28</sup> differences in core sizes following electron transfer may thus modulate the interaction between the metal-NO unit and the macrocycle. Strauss et al.<sup>27</sup> have similarly suggested that changes in core sizes alter the affinity of iron complexes for  $\sigma$ -donors.

Controlled-potential electrolyses of Co-NO P, C, and iBC require 1 ( $\pm 0.1$ ) electron to yield the optical spectra shown in Figures 1 and 2. The oxidized species are stable and one-electron reductions regenerate the starting nitrosyl compounds.

That the NO ligands are retained in the oxidized Co species is confirmed by infrared data: NO stretches (Nujol nulls) are observed at  $1700\text{ cm}^{-1}$  for OEP and MeOEC and at  $1695\text{ cm}^{-1}$  for 2,3-DMeOEiBC (confirmed with  $^{15}\text{NO}$  in the latter case:  $\nu_{^{15}\text{NO}} = 1665\text{ cm}^{-1}$ ). The NO frequencies are readily distinguishable from those of the unoxidized compounds:  $\nu_{\text{NO}} = 1660\text{ cm}^{-1}$  in P and C and  $1655\text{ cm}^{-1}$  in iBC. The Co-NO bond of  $\text{CoTPPNO}$  has been shown to be bent by X-ray analysis with  $\nu_{\text{NO}} = 1689\text{ cm}^{-1}$  in KBr.<sup>29</sup> The NO stretches reported here are comparable

(24) Fujita, E.; Fajer, J., unpublished results. The trend applies for the oxidations of  $\text{Co}^{\text{III}}$  but not  $\text{Co}^{\text{II}}\text{P}$ , C, and iBC in several coordinating and noncoordinating solvents.

(25) Kelly, S.; Lancon, D.; Kadish, K. M. *Inorg. Chem.* **1984**, *23*, 1451-1458.

(26) The reduced  $\text{Co}^{\text{II}}\text{NOEiBC}$  is paramagnetic and, at 123 K in butyronitrile, exhibits a broad, cobalt ESR signal, over 1000 G wide, that differs from that of  $\text{Co}^{\text{II}}\text{OEiBC}$ . Details of this work will be presented elsewhere.

(27) Strauss, S. J.; Silver, M. E.; Ibers, J. A. *J. Am. Chem. Soc.* **1983**, *105*, 4108-4109.

(28) Barkigia, K. M.; Fajer, J.; Spaulding, L. D.; Williams, G. J. B. *J. Am. Chem. Soc.* **1981**, *103*, 176-181. Barkigia, K. M.; Fajer, J.; Chang, C. K.; Williams, G. J. B. *Ibid.* **1982**, *104*, 315-317. Barkigia, K. M.; Fajer, J.; Chang, C. K.; Young, R. *Ibid.* **1984**, *106*, 6457-6459 and references therein.

(29) Scheidt, W. R.; Hoard, J. L. *J. Am. Chem. Soc.* **1973**, *95*, 8281-8286.

to that value, and the Co-NO bonds are thus assumed also to be bent in the parent as well as the oxidized compounds.

CoOEPNOCIO<sub>4</sub> also exhibits an IR band at 1560 cm<sup>-1</sup>, a frequency considered diagnostic of OEP  $\pi$ -cation radicals by Shimomura et al.<sup>30</sup>

The optical spectra of the oxidized compounds presented in Figures 1 and 2 also display features typical of  $\pi$  radicals of their respective species: weaker Soret bands, and bleaching of the visible bands accompanied by broad, featureless absorption stretching into the near-infrared.<sup>7,8,15-17</sup> The porphyrin spectrum (Figure 1) is similar to that assigned to a<sub>2u</sub> radicals.<sup>16,17</sup> Such radicals are characterized by significant spin densities at the pyrrole nitrogens, the meso positions, the metal, and the axial ligand.<sup>14,16,17,31</sup> The ESR spectrum observed at room temperature in CH<sub>2</sub>Cl<sub>2</sub> for CoNOOEP<sup>+</sup>ClO<sub>4</sub><sup>-</sup>, a singlet line with  $\Delta H_{pp} = 30$  G, is consistent with an a<sub>2u</sub> assignment but yields no details of the spin distribution in the radical; attempts to obtain solution ENDOR data have been unsuccessful so far.<sup>32</sup> The ESR spectrum of the porphyrin nitrosyl radical is distinct from that of Co<sup>III</sup>OEP(ClO<sub>4</sub>)<sub>2</sub> and, combined with the observed NO stretch, minimizes the possibility that oxidation has resulted in loss of NO followed by generation of the Co<sup>III</sup> radical. (Such a reaction has been proposed by Kelly et al.<sup>24</sup> to explain the characteristic radical optical spectrum observed on oxidation of CoTPPNO. The OEP results suggest the formation of the analogous CoTPPNO<sup>+</sup>.)

The radical nature of the oxidized CoNOC and iBC is evident from their ESR signals (Figures 3 and 4). A<sub>1u</sub> states are predicted for such C and iBC cations, with characteristic high-spin densities at the  $\alpha$  carbons of the pyrroles, that are reflected experimentally by large coupling constants for the  $\beta$  protons on the saturated rings (4–8 G), and small nitrogen splittings (~0.5–1 G).<sup>5,8,14-16</sup> The 3 isomers of DMeOEiBC allow the  $\alpha$  carbons of the saturated rings to be sampled via the  $\beta$  protons and have previously been used to verify the predicted a<sub>1u</sub> spin distribution of free base, zinc, and Fe<sup>II</sup>CO iBC radicals.<sup>8</sup> The simulations shown in Figure 3 demonstrate that two protons ( $a_H = 4.5$  and 6.7 G) and one cobalt ( $a_{Co} = 2.7$ –2.8 G) determine the spectral patterns observed for the Co<sup>II</sup>NOiBC<sup>+</sup> radicals.<sup>33</sup> The proton coupling constants are comparable to those found in other radicals of the same macrocycle<sup>8</sup> ( $a_H = 4.6$ –5.0 and 6.8–7.4 G). The CoNOiBC<sup>+</sup>'s thus fit a<sub>1u</sub> profiles but do require some interaction with the metal. The nitrosyl chlorins yield similar results as shown in Figure 4. The spectra require contributions from the protons of the saturated rings ( $a_H = 4.0$  and 7.1 G<sup>34</sup>) and an additional interaction with

the cobalt,  $a_{Co} = 3.3$  G, as in the iBC radicals. The proton coupling constants are again comparable to those found in other complexes of the same macrocycles ( $a_H = 4.6$  and 7.25 G for ZnOEC<sup>+</sup><sup>35</sup> and ZnMeOEC<sup>+</sup>,<sup>16</sup> respectively) and are typical values expected for a<sub>1u</sub> radicals.<sup>14-16</sup>

The comparisons between the iron and cobalt-nitrosyl species thus indicate (a) that the Co complexes are harder to reduce than the Fe ones by a constant 0.18 V for the 3 macrocycles, suggestive of electron addition to the Co or NO; and (b) the Co-NO porphyrin is harder to oxidize than the corresponding iron compound by 0.14 V but the Co-NO and Fe-NO C and iBC complexes oxidize at nearly the same potentials ( $\pm 0.02$  V). This accords with the assignments of ring oxidation for the C and iBC complexes of both metals, and with the metal (Fe<sup>III</sup>NOP<sup>+</sup>) vs. ring (Co<sup>II</sup>NOP<sup>+</sup> radical) oxidations in the case of the Fe and Co porphyrins. The stability of the metal-nitrosyl bonds as well as their configuration (linear or bent) also varies with the metal and the oxidation state. Substitution of cobalt for iron in a biological system could thus offer additional modes of controlling sites of oxidation, redox potentials, and the reactivity or stability of the resulting species.

Experimental electronic profiles for other hydroporphyrin radicals such as chlorophylls, bacteriochlorophylls, and bacteriochlorins<sup>14-16,36,37</sup> agree well with predominantly a<sub>1u</sub> distributions. These results conform with MO calculations as varied as extended Hückel,<sup>15,16</sup> SCF Pariser-Parr-Pople,<sup>14</sup> INDO,<sup>37</sup> and molecular fragment ab initio.<sup>38</sup> The present ESR results further support the a<sub>1u</sub> profiles calculated<sup>8,15,16</sup> for C and iBC cations and thus lend additional credence to predicted a<sub>1u</sub> distributions<sup>8,16</sup> for the increasing number of hydroporphyrins being assigned biological functions.<sup>2,3,12,39</sup>

A<sub>1u</sub> and a<sub>2u</sub> porphyrin radicals have long been invoked in the oxidation cycles of catalases and peroxidases<sup>17</sup> and in synthetic catalysts modelled<sup>40</sup> on the mechanisms postulated for these enzymes and cytochrome P450. MO calculations<sup>16,41</sup> favor a<sub>1u</sub> states for heme radicals with axial ligands such as tyrosine (catalase) or thiolates (chloroperoxidase and P450), as opposed to a<sub>2u</sub> configurations<sup>16,39</sup> for the imidazole-ligated heme of horseradish peroxidase. ESR and ENDOR studies<sup>42</sup> of the oxidized compound I of the latter, isotopically substituted with <sup>17</sup>O, <sup>2</sup>H, and <sup>15</sup>N, support the a<sub>2u</sub> assignment for that intermediate. However, ESR results for compound I of chloroperoxidase were judged<sup>18</sup> inconsistent with its predicted<sup>16,41</sup> a<sub>1u</sub> character because magnetic coupling between the metal and the P radical was not expected in a<sub>1u</sub> radicals. The chlorin and isobacteriochlorin cobalt-nitrosyl radicals discussed above clearly exhibit a<sub>1u</sub> characteristics and further belong to general classes of hydroporphyrins that have repeatedly been shown to conform to a<sub>1u</sub> profiles. Nonetheless, the Co-NO a<sub>1u</sub> radicals unambiguously display magnetic interactions between the metals and their complexing macrocycles and thus demonstrate that such couplings are indeed possible, at least in some a<sub>1u</sub> radicals. The reason for this effect may lie in the small amount of negative spin density that is found on the nitrogen atoms of hydroporphyrin radicals<sup>36,37,43</sup> which would allow coupling to the metal, as in a<sub>2u</sub> porphyrin radicals.<sup>14</sup> (Co hyperfine constants reported for well-characterized a<sub>2u</sub>

(30) Shimomura, E. T.; Phillippi, M. A.; Goff, H. M.; Scholz, W. F.; Reed, C. A. *J. Am. Chem. Soc.* **1981**, *103*, 6778–6780.

(31) Ohya-Nishiguchi, H.; Kohno, M.; Yamamoto, K. *Bull. Chem. Soc. Jpn.* **1981**, *54*, 1923–1927.

(32) The experimental ESR spectrum of CoOEPNO<sup>+</sup> can be approximated by using coupling constants estimated from other a<sub>2u</sub> Co  $\pi$  radicals:<sup>14,31</sup>  $a_{Co} \sim 3.5$ –4 G,  $a_N(\text{pyrroles}) \sim 2$  G,  $a_H(\text{meso}) \sim 5$  G, and  $a_N(\text{NO}) \sim 1$ –2 G. Upon deuteration of the meso positions,  $\Delta H_{pp}$  for CoOEP(d<sub>4</sub>)NO<sup>+</sup> decreases to 27 G, in accord with significant delocalization of the unpaired electron onto the macrocycle and in agreement with the estimated coupling constants for the meso positions.

(33) Substitution of <sup>15</sup>NO for <sup>14</sup>NO has no obvious effect on the experimental spectra.

(34) While the two proton coupling constants observed experimentally in the iBC radicals reflect the different spin densities predicted for the inboard and outboard  $\alpha$  carbons of the saturated rings, the very different proton constants of the two nearly identical chlorins probably do not arise from different spin densities at the  $\alpha$  carbons but from different torsional angles imposed on the saturated ring by  $\beta$  substituents. The observed coupling constant of a  $\beta$  proton,  $a_H$ , is defined<sup>14</sup> by  $a_{H\beta} = (\text{constant})\rho_c(\cos^2 \theta)$  where  $\rho_c$  is the spin density at the  $\alpha$  carbon and  $\theta$  is the dihedral angle defined by the plane C <sub>$\alpha$</sub> C <sub>$\beta$</sub> H <sub>$\beta$</sub>  and the p<sub>z</sub> orbital of C <sub>$\alpha$</sub> . Significant changes in observed coupling constants can thus be induced for the same  $\rho$  value by changing  $\theta$ . X-ray data for several chlorins show a range of  $\theta$  values in accord with the trend observed by ESR, i.e.,  $\theta$  is smaller in the compounds with the larger  $a_{H\beta}$  values. (Barkigia, K. M.; Fajer, J., unpublished results.) The fact that the Co coupling constants are the same in the two Co<sup>II</sup>NO chlorins further suggests that the overall spin distributions in the two radicals are indeed similar.

(35) Fujita, E.; Fajer, J., unpublished results.

(36) Fajer, J.; Davis, M. S.; Brune, D. C.; Spaulding, L. D.; Borg, D. C.; Forman, A. *Brookhaven Symp. Biol.* **1976**, *28*, 74–104.

(37) Lendzian, F.; Mobius, K.; Plato, M.; Smith, U. H.; Thurnauer, M. C.; Lubitz, W. *Chem. Phys. Lett.* **1984**, *111*, 583–588 and references therein.

(38) Petke, J. D.; Maggiora, G. M.; Shipman, L. L.; Christoffersen, R. E. *Photochem. Photobiol.* **1980**, *31*, 243–257.

(39) Andersson, L. A.; Loehr, T. M.; Chang, C. K.; Mauk, G. A. *J. Am. Chem. Soc.* **1985**, *107*, 182–191 and references therein.

(40) Goff, H. M.; Phillippi, M. A. *J. Am. Chem. Soc.* **1983**, *105*, 7567–7573. Groves, J. T.; Haushalter, R. C.; Nakamura, M.; Nemo, T. E.; Evans, B. J. *Ibid.* **1981**, *103*, 2884–2886.

(41) Fujita, I.; Hanson, L. K.; Walker, F. A.; Fajer, J. *J. Am. Chem. Soc.* **1983**, *105*, 3296–3300.

(42) Roberts, J. E.; Hoffman, B. M.; Rutter, R.; Hager, L. P. *J. Biol. Chem.* **1981**, *256*, 2118–2121. Roberts, J. E.; Hoffman, B. M.; Rutter, R.; Hager, L. P. *J. Am. Chem. Soc.* **1981**, *103*, 7654–7656.

(43) Lubitz, W.; Isaacson, R. A.; Abresh, E. C.; Feher, G. *Proc. Natl. Acad. Sci. U.S.A.* **1984**, *81*, 7792–7796.

Co<sup>III</sup>P<sup>2+</sup> radicals average<sup>14,31</sup> ~6-7 G to be compared with the ~3 G found here in the a<sub>1u</sub> Co species.) Negative spin densities at the nitrogen atoms, expected for a<sub>1u</sub> porphyrins,<sup>14</sup> or some admixture of a<sub>2u</sub> character,<sup>16,44</sup> may provide the mechanism that

(44) Morishima, I.; Takamuki, Y.; Shiro, Y. *J. Am. Chem. Soc.* **1984**, *106*, 7666-7672.

couple metal and radical in compounds I of chloroperoxidase and other presumed a<sub>1u</sub> species.

**Acknowledgment.** This work was supported by the Division of Chemical Sciences, U.S. Department of Energy (Contract DE-AC02-76CH00016) at Brookhaven National Laboratory and by the National Science Foundation at Michigan State University.

## Biomimetic Models for Cysteine Proteases. 3. Acylation of Imidazolium-Thiolate Zwitterions by *p*-Nitrophenylacetate as a Model for the Acylation Step and Demonstration of Intramolecular General-Base-Catalyzed Delivery of H<sub>2</sub>O by Imidazole to Thiol Esters as a Model for the Deacylation Step

J. P. Street,<sup>†</sup> K. I. Skorey,<sup>†</sup> R. S. Brown,<sup>\*†</sup> and R. G. Ball<sup>‡</sup>

Contribution from the Department of Chemistry, University of Alberta, Edmonton, Alberta, Canada, T6G 2G2, and the Structure Determination Laboratory, Department of Chemistry, University of Alberta, Edmonton, Alberta, Canada, T6G 2G2. Received April 19, 1985

**Abstract:** As biomimetic models for the cysteine proteases, four imidazole-thiol pairs, 4(5)-(mercaptomethyl)imidazole (**1a**), 2-(mercaptomethyl)imidazole (**2a**), 2-(mercaptomethyl)-*N*-methylimidazole (**3a**), and 2-(4,5-dimethylimidazol-2-yl)benzenethiol (**4a**) are studied as a function of pH as to their propensity to attack *p*-NPA and dinitrophenylacetate (for **4a**). All species (except **1a**) attack through their thiolate forms and show a plateau region at intermediate pH values which is attributable to attack by the thiolate anion of the zwitterionic forms (ImH<sup>+</sup>-S<sup>-</sup>). **1a** attacks as its thiolate at high pH and through imidazole N at neutrality. Potentiometric and UV-visible spectrophotometric titrations establish quantitatively the microscopic pK<sub>a</sub> values from which are derived the fraction of individual species at any pH. General-base assistance of thiol attack on the acylating agent by the proximal imidazole is not required to explain the result. Deacylation of the corresponding thiol esters **1c-4c** is studied as a function of pH, and in all cases, a plateau region from pH 6.5-7 to 8.5-10 is observed. Solvent deuterium isotope effects from 1.88 (**1c**) to 3.75 (**4c**) are observed at neutral pH values. In all cases, the origin of the plateau region stems from a general-base-promoted delivery of H<sub>2</sub>O to the thiol ester by the proximal imidazole. Trapping experiments with Ellman's reagent suggest that S- → N-acyl transfer is not an important process for these systems. The relevance of these findings is discussed in terms of the mechanism of action of the cysteine proteases.

### I. Introduction

The cysteine proteases form a large class of enzymes from plant, animal, and bacterial sources,<sup>1,2</sup> the active sites containing both an essential cysteine SH and histidine-imidazole unit.<sup>3</sup> Although the natural function of the plant enzymes is unknown, their robust character and relative ease of isolation make them commercially valuable<sup>4</sup> as proteolytic agents.

While the detailed mechanism of action is uncertain, papain and other cysteine proteases cleave both ester and amide substrates with the intermediacy of an *S*-acyl-enzyme.<sup>1,5</sup> For ester substrates, the deacylation step is predominantly rate-limiting, while for amides the acylation step is.<sup>6</sup>

The possible sequences for papain-mediated hydrolyses are given in a highly stylized fashion in Figure 1. Early work<sup>7</sup> showed that the pH vs. rate profile for acyl-enzyme formation from a typical ester (*N*-benzoyl-L-arginine ethyl ester (BAEE)) or amide ( $\alpha$ -*N*-benzoyl-L-arginamide (BAA)) substrate was bell-shaped and dependent on two groups having apparent pK<sub>a</sub> values of ~3.9-4.3 and 8.2-8.5. The former value was originally<sup>7b,8</sup> attributed to a carboxylate residue but was later changed to an imidazolium group;<sup>9</sup> the second pK<sub>a</sub> was attributed to the Cys-SH. The general scheme for acylation (Figure 1) was then suggested to involve a general-base role for the imidazole in assisting thiol attack.<sup>9</sup>

However, the most recent evidence from spectral and potentiometric titration as well as from solvent isotope effects<sup>18,10</sup> indicates that in papain, Cys-25 has an unusually low pK<sub>a</sub> of 3-4

while that of His-159 is 8.5. It is proposed<sup>10a</sup> that at physiological pH, 90% of the papain exists in a form wherein the active site

(1) (a) Glazer, A. N.; Smith, E. L. In "The Enzymes"; Boyer, P. D., Ed.; Academic Press: New York, 1971, Vol. 3, pp 502-546. (b) Drenth, J.; Jansonius, J. N.; Koekoek, R.; Wolthers, B. G. *Ibid.* 1971, Vol. 3, pp 484-499. (c) Liu, T.-Y.; Elliott, S. D. *Ibid.* 1971, Vol. 3, pp 609-647. (d) Mitchell, W. M.; Harrington, W. F. *Ibid.* 1971, Vol. 3, pp 699-719. (e) Brocklehurst, K. *Methods Enzymol.* **1982**, *87c*, 427. (f) Polgar, L.; Halász, P. *Biochem. J.* **1982**, *207*, 1. (g) Drenth, J.; Kalk, K. H.; Swen, H. M. *Biochemistry* **1976**, *15*, 3731.

(2) (a) Wong, R. C.; Liener, I. E. *B.B.R.C.* **1964**, *17*, 470. (b) Husain, S. S.; Lowe, G. *J. Chem. Soc., Chem. Commun.* **1966**, 1387. (c) Baker, E. N. *J. Mol. Biol.* **1977**, *115*, 263; **1980**, *141*, 441. (d) Tsunada, J. N.; Yasunobu, K. T. *J. Biol. Chem.* **1966**, 4610.

(3) (a) Boland, M. J.; Hardman, M. J. *FEBS Lett.* **1972**, *27*, 282. (b) Boland, M. J.; Hardman, M. J. *Eur. J. Biochem.* **1973**, *36*, 575. (c) Hussain, S. S.; Lowe, G. *Biochem. J.* **1968**, *108*, 855.

(4) (a) Levens, S. M.; Gruber, D. K.; Gruber, C.; Lent, R.; Seifter, E. *J. Trauma* **1981**, *21*, 632 (debridement of burns as a pretreatment for skin grafts). (b) Taussig, S. J.; Yokoyama, M. M.; Chinen, A.; Onari, K.; Yamakido, M.; Nishimoto, Y. *Hiroshima J. Med. Sci.*, **1975**, *24*, 185. (c) A well-known Mexican skin tonic consists of rubbing the facial skin with papaya rind to give a "youthful fresh appearance"; Briskin, M.; Briskin, L. S. In "Make Your Own Cosmetics"; Dell Publishing Co.: New York, 1971; p 63. (d) Commercial meat tenderizing agents list papain (papain) as their active ingredient.

(5) (a) Wilson, I. B.; Bergmann, F.; Nachmansohn, D. *J. Biol. Chem.* **1950**, *186*, 781. (b) Weisz, J. *Chem. Ind. (London)* **1937**, *15*, 685. (c) Lowe, G.; Williams, A. *Biochem. J.* **1965**, *96*, 189. (d) Storer, A. C.; Murphy, W. F.; Carey, P. R. *J. Biol. Chem.* **1979**, *254*, 3163. (e) Brocklehurst, K.; Cook, E. M.; Wharton, C. W. *J. Chem. Soc., Chem. Commun.* **1967**, 1185. (f) Brubacker, L. J.; Bender, M. C. *J. Am. Chem. Soc.* **1964**, *86*, 5333. (g) Smolarski, M. *Isr. J. Chem.* **1974**, *12*, 615. (h) Malthouse, J. P. G.; Gamszik, M. P.; Boyd, A. S. F.; Mackenzie, N. E.; Scott, A. I. *J. Am. Chem. Soc.* **1982**, *104*, 6811. (i) Lowe, G. *Tetrahedron* **1976**, *32*, 291.

<sup>†</sup> Department of Chemistry.

<sup>‡</sup> Structure Determination Laboratory, Department of Chemistry.